



A review of multivariate methods of analysing refractive data with dioptric power matrices



Authors:

Elizabeth Chetty¹ 
Alan Rubin¹ 

Affiliations:

¹Department of Optometry,
Faculty of Health Sciences,
University of Johannesburg,
Johannesburg, South Africa

Corresponding author:

Elizabeth Chetty,
echetty@uj.ac.za

Dates:

Received: 18 Oct. 2021

Accepted: 04 Aug. 2022

Published: 08 Nov. 2022

How to cite this article:

Chetty E, Rubin A. A review of multivariate methods of analysing refractive data with dioptric power matrices. *Afr Vision Eye Health*. 2022;81(1), a714. <https://doi.org/10.4102/aveh.v81i1.714>

Copyright:

© 2022. The Author(s).
Licensee: AOSIS. This work is licensed under the Creative Commons Attribution License.

Background: There are three components to refractive state, namely sphere, cylinder and axis. Similarly, central corneal power is also composed of three components, namely the power along the flat meridian, the power along the steep meridian and the axis of the flat meridian. Most studies that investigate refractive data and corneal power analyse each of the three components individually rather than as a trivariate entity. In doing so, pertinent information may inadvertently be omitted.

Aim: The purpose of this review is to provide a brief overview of the multivariate statistics that are available to analyse multivariate data such as dioptric power. This will enable readers to better understand research that is analysed using these methods.

Method: An extensive review of databases such as Google Scholar, Science Direct and ResearchGate was done to gather publications on the topic of multivariate statistical analysis. Keywords such as multivariate statistical analysis, dioptric power, stereo-pairs, polar profiles and hypothesis testing were used to conduct the search.

Results: The debate for the need to analyse dioptric power using multivariate statistical methods has been a long-standing one. For this review, more than 40 publications were analysed to provide a simplified overview of the multivariate statistical methods that can be used to analyse dioptric power.

Conclusion: The use of multivariate statistical methods is a valuable tool in analysing and understanding dioptric power holistically and may provide more insights for research involving refractive error and corneal power.

Keywords: multivariate statistical analysis; dioptric power space; dioptric power; stereo-pairs; polar profiles; hypothesis testing.

Introduction

Multivariate statistical analysis provides a method to analyse the trivariate nature of dioptric power holistically, thus enabling one to evaluate the scalar (spherical) as well as the astigmatic changes that may occur. In earlier literature, the scalar axis was referred to as the stigmatic axis. Treating sphere, cylinder and axis as a univariate entity (spherical equivalent) diminishes the meaningfulness of conclusions drawn because astigmatic changes that may occur are diluted thereby. With the multivariate transformation of dioptric power, standard statistical calculations such as means, standard deviations and variances can be determined thus making hypothesis testing possible. Around the late seventies, the idea of analysing dioptric power with multivariate statistics was conceptualised by researchers such as Long,¹ Keating^{2,3,4} and Harris.⁵ Over the decades, work done by Harris^{5,6,7,8,9,10,11,12,13,14,15,16,17,18,19,20,21,22,23,24,25} and others including Thibos et al.,²⁶ for example, led to the development of the multivariate methods of analysis that are available today to analyse dioptric power in its entirety. The matrix representation of dioptric power and the ability to add, average and square spherocylindrical powers allows for variances and standard deviations, as well as other multivariate statistics, to be calculated,⁶ which were thought to be impossible for such data.²⁷ These methods of analysing refractive and keratometric data have been used frequently in research,^{28,29,30,31,32,33,34} and the aim of this review is to provide a simplified overview of the multivariate methods of analysis of dioptric power so that readers of such research can better understand the analysis used in those studies. The data used in the examples provided are measurements taken on patients with keratoconus (KC). There have not been many other studies done on KC patients using this sort of analysis.

Read online:



Scan this QR code with your smart phone or mobile device to read online.

The matrix representation of dioptric power

A $m \times n$ matrix (m rows by n columns) is a linear algebra mathematical concept defined by a set of entries or elements placed in a specific arrangement. According to Harris,⁵ credit should go to H Fick³⁵ and W.F. Long¹ who pioneered the idea that dioptric power could be expressed as a 2×2 matrix. For sphero-cylindrical power, this 2×2 matrix is symmetric; that is, the off-diagonal entries are equal; therefore, there are only three distinct numbers just as there are three numbers (sphere, cylinder and axis) representing dioptric power in clinical notation. The unit of measurement of the dioptric power matrix is dioptres or inverse metres (m^{-1}), whereas the unit of measurement for a sphero-cylinder is a combination of dioptres (for sphere and cylinder power) and degrees (for axis). Consider the following 2×2 matrix:

$$\mathbf{F} = \begin{bmatrix} f_{11} & f_{12} \\ f_{21} & f_{22} \end{bmatrix}. \quad [\text{Eqn 1}]$$

The positions of the elements, or entries, are described by the subscripts. The first number in the subscript defines the row and the second number defines the column in which the element is positioned. For example, f_{11} is the entry in row 1 and column 1, f_{21} is the entry in row 2 and column 1. Each entry in the dioptric power matrix represents a particular characteristic of the dioptric power from which it was converted. The entries f_{11} and f_{22} link back directly to the curvital power in the horizontal and vertical meridians, respectively, while f_{12} , which for a symmetric matrix is equal to f_{21} , represents the torsional component of refractive power.^{5,12}

A set of formulae, which were derived to convert sphero-cylindrical powers to a dioptric power matrix and *vice versa* are outlined. For conversion from clinical notation (sphere, cylinder and axis) to matrix representation¹:

$$f_{11} = F_s + F_c \sin^2 a \quad [\text{Eqn 2}]$$

$$f_{12} = f_{21} = -F_c \sin a \cos a \quad [\text{Eqn 3}]$$

$$f_{22} = F_s + F_c \cos^2 a \quad [\text{Eqn 4}]$$

where F_s is sphere (D), F_c is cylinder (D) and a is axis (degrees).

Conversion from matrix representation to clinical notation (sphere, cylinder and axis)²:

$$F_c = -\sqrt{t^2 - 4d} \quad [\text{Eqn 5}]$$

$$F_s = (t - F_c) / 2 \quad [\text{Eqn 6}]$$

$$\tan a = (F_s - f_{11}) / f_{12} \quad [\text{Eqn 7}]$$

where t is the trace and d is the determinant and are defined by

$$t = f_{11} + f_{22} \quad [\text{Eqn 8}]$$

and

$$d = f_{11}f_{22} - f_{12}f_{21}, \quad [\text{Eqn 9}]$$

respectively.

These equations work well for thin systems that meet the requirements when analysing clinical sphero-cylindrical data. However, thick systems, for example, the power of the human eye, are more complicated and require a distinct fourth element in the 2×2 matrix thereby rendering it asymmetric. This matter is beyond the scope of this overview and the interested reader is referred elsewhere.^{3,17,20,21,22}

The matrix is an orthodox mathematical concept; therefore, the whole field of linear algebra (matrix algebra) becomes available. With sphero-cylindrical power having a mathematical representation (the dioptric power matrix), any mathematical function is thus possible with refractive or keratometric data including calculating means and variances, which are two paramount statistics when comparing samples of data and making inferences for populations.¹¹ All the statistical methods discussed in this review are based on the dioptric power matrix. Harris, Malan and Rubin^{36,37,38,39,40,41} contributed to the development of mathematical, statistical and software methods that were specifically designed to convert such data into matrix representations for multivariate statistical analyses. Refractive powers and corneal powers can be converted into matrices so that they can be plotted in three-dimensional symmetric dioptric power space. Thereafter all the statistical functions and methods required to analyse the data are carried out on the matrix equivalents. For corneal power, raw keratometric data (radii of curvature along principal meridians) must first be converted into conventional powers using a nominal refractive index (usually 1.3375) and then into matrix representations. For the purposes of demonstrating the usefulness of the multivariate methods of analysis, the first author has used figures generated from data that were collected during her postgraduate doctoral studies.⁴¹ Central corneal power measurements were obtained for a sample of keratoconic and healthy control eyes and thereafter compared.

Stereo-pair scatter plots

Multivariate statistical analysis of dioptric power is based on assumptions such as data normality and equality of variances, and if these assumptions are violated for a particular sample, then the inferences made on such data need to be treated with caution. However, if that data were to be represented graphically, then the statistical inferences should be validated so that the conclusions drawn would be more meaningful.¹⁵

Stereo-pair scatter plots provide a visual representation of dioptric power in its entirety without any underlying assumptions thus providing graphical substantiation to all statistical assertions made in a study. Each point in a scatter plot represents one refractive power or one corneal power that was converted from its sphero-cylindrical form to a matrix that is plotted in three-dimensional Euclidean space.¹⁶ Thibos and others²⁶ use vectors to perform similar analyses

but without stereo-pairs that can be useful in enhancing data visualisation and analysis.

Work by Harris on representing dioptric power graphically evolved over the years to overcome shortcomings he found along the way.^{15,16,21,22} This led to the development of a four-dimensional space called dioptric power space for thick optical systems but which also has symmetric dioptric powers representing thin optical systems.^{16,21} Symmetric dioptric power space is the three-dimensional sub-space, which represents sphero-cylindrical powers such as those commonly analysed in optometric and ophthalmologic research.

Harris^{22,23,24,25} represents symmetric dioptric power as:

$$\mathbf{F} = F_I \mathbf{I} + F_J \mathbf{J} + F_K \mathbf{K} \quad (\text{or} = F_{st} \mathbf{I} + F_{or} \mathbf{J} + F_{ob} \mathbf{K}) \quad [\text{Eqn } 10]$$

also written as

$$\mathbf{F} = \mathbf{F}_I + \mathbf{F}_J + \mathbf{F}_K \quad (\text{or} = \mathbf{F}_{st} + \mathbf{F}_{or} + \mathbf{F}_{ob}) \quad [\text{Eqn } 11]$$

or as a coordinate vector

$$\mathbf{f} = \begin{bmatrix} F_I \\ F_J \\ F_K \end{bmatrix} \quad \text{or} \quad \mathbf{v} = \begin{bmatrix} F_{st} \\ F_{or} \\ F_{ob} \end{bmatrix} \quad [\text{Eqn } 12]$$

where \mathbf{I} , \mathbf{J} and \mathbf{K} represent the basis matrices $\begin{bmatrix} 1 & 0 \\ 0 & 1 \end{bmatrix}$, $\begin{bmatrix} 1 & 0 \\ 0 & -1 \end{bmatrix}$ and $\begin{bmatrix} 0 & 1 \\ 1 & 0 \end{bmatrix}$, respectively, and $F_I (= F_{st})$, $F_J (= F_{or})$ and $F_K (= F_{ob})$ are scalars defined by:

$$F_I = \frac{1}{2} (f_{11} + f_{22}) = F_s + \frac{1}{2} F_c \quad [\text{Eqn } 13]$$

$$F_J = \frac{1}{2} (f_{11} - f_{22}) = -\frac{1}{2} F_c \cos 2a \quad [\text{Eqn } 14]$$

$$F_K = \frac{1}{2} (f_{21} + f_{12}) = -\frac{1}{2} F_c \sin 2a. \quad [\text{Eqn } 15]$$

The unit of measurement for the scalars F_{st} , F_{or} and F_{ob} is dioptres; however, the matrices \mathbf{I} , \mathbf{J} and \mathbf{K} do not have units. More recently, F_I , F_J and F_K are used for F_{st} , F_{or} and F_{ob} , respectively. The scalar quantities here are the same as M , J_0 and J_{45} of Thibos and others.²⁶

$F_I \mathbf{I}$, $F_J \mathbf{J}$ and $F_K \mathbf{K}$ (or F_I , F_J and F_K , respectively) are matrices that can be graphed along three mutually orthogonal axes (in three-dimensional dioptric power space), that is, axes along which any dioptric power can be plotted (see Figure 1 for an example of stereo-pairs with 95% distribution ellipsoids [discussed later]). $F_I \mathbf{I}$ is the scalar axis and represents the spherical component of power. The plane orthogonal to the $F_I \mathbf{I}$ axis is the plane of all Jackson cross cylinder (JCC) powers or symmetric antistigmatic powers. This plane comprises the ortho-antistigmatic powers ($F_J \mathbf{J}$) with principal meridians along 0° and 180° and the oblique antistigmatic powers ($F_K \mathbf{K}$) with principal meridians along 45° and 135° . The antistigmatic plane in which the two antistigmatic axes are found contains all powers that are JCC.

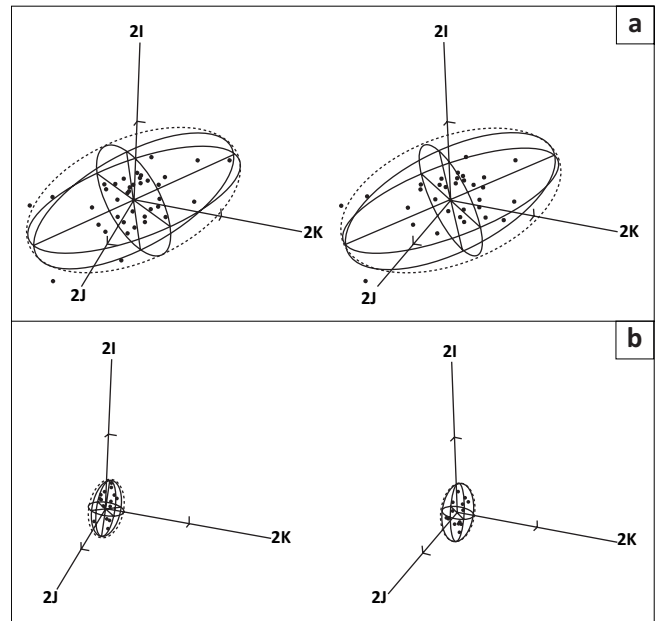


FIGURE 1: Stereo-pair scatter plots with 95% distribution ellipsoids of (a) 40 consecutive central corneal power measurements taken on a single keratoconic eye and (b) 40 consecutive central corneal power measurements taken on a single control eye.⁴¹ The stereo-pairs have an axis length of 2 D and a tick interval of 1 D. The origin is placed at the sample mean for each stereo pair.

Variation in this plane represents variation in JCC powers, which is a type of astigmatic variation. More completely, however, astigmatic variation includes any variation in symmetric dioptric power space that excludes variation along the scalar axis only. To appreciate the three-dimensional nature of the data in the stereo-pairs, one is required to let one's eyes drift into an exo- or eso-position. Using this sort of graphical representation of dioptric power makes it easy to make comparisons between two or more samples. For example, Figure 1a represents 40 consecutive central corneal power measurements taken on a single keratoconic eye, and Figure 1b represents 40 consecutive central corneal power measurements taken on a single healthy control eye. Immediately, one can see that there is greater variation in corneal power in the eye with KC when compared to the healthy eye. Another observation easily made is that the variation within the keratoconic eye is predominantly astigmatic or antistigmatic (the data points are scattered mostly along a direction near the antistigmatic plane that contains the other two axes), whereas the variation within the control eye is predominantly stigmatic (the data points are mostly scattered along the scalar axis with label 2I).

Ellipsoids

An ellipsoid is the three-dimensional equivalent of an ellipse. For the purposes of this review, $\alpha = 0.05$ therefore samples of dioptric power data can be used to generate 95% ellipsoids of constant probability density and 95% confidence ellipsoids for means. Other values can be used for α , which result in change in size and volume; however, the shape and orientation of the ellipsoid are maintained. The principal diameters and principal radii of an ellipsoid are measured along its three mutually orthogonal principal axes. The directions of these axes provide useful information when

making comparisons between samples or populations. Every ellipsoid has a centroid or centre (the sample mean). The position of the centroid is maintained regardless of the α used.^{15,16}

Ellipsoids of constant probability density

In multivariate statistics, analysis done on a random and normally distributed sample can be used to make inferences on the population from which the sample was obtained. A sample of dioptric powers can be used to generate ellipsoids of constant probability density (also referred to as distribution ellipsoids), which provide a graphical representation of the spread of dioptric power in a sample. The size, shape and orientation of these distribution ellipsoids characterise the nature of the variation of the population and provide a visual aid in making comparisons between populations.¹⁶ As can be seen from Figure 1, these distribution ellipsoids provide a visual indication of the nature of the variation of the dioptric power within the sample. One is able to easily identify differences between eyes with KC and control eyes by comparing the sizes, shapes and orientations of the distribution ellipsoids generated for different samples.⁴¹

Confidence ellipsoids

While ellipsoids of constant probability density describe the distribution of the population of, for example, dioptric power measurements, confidence ellipsoids are confidence regions centred on the sample mean.^{15,16} Confidence ellipsoids also provide an estimation of the mean of the population. Therefore, for example, one can assume at a 95% level of confidence that the mean of a particular population of dioptric power measurements will lie within the respective 95% confidence ellipsoid. Confidence ellipsoids also demonstrate the accuracy of the mean, that is, the smaller the 95% confidence ellipsoid, the less variation is exhibited by the sample and the more confident one can be about the accuracy of the mean. If the confidence ellipsoids of two samples being compared do not intersect (Figure 2a), then one can argue at a known level of confidence (e.g. a 95% level of confidence more specifically) that a change in means did occur.¹⁷ The opposite applies when the confidence ellipsoids do intersect (Figure 2b). However, formal hypothesis tests^{15,17,19} are used to compare the variances and also means for the two samples concerned.

Means and variances and covariances of dioptric power

Adapted from Harris^{11,12,13,14,15,16,17}; the average of a sample of n powers F_i is given by:

$$\bar{F} = \frac{1}{n} \sum_{i=1}^n F_i \quad [\text{Eqn 16}]$$

The transpose of equation 12 is:

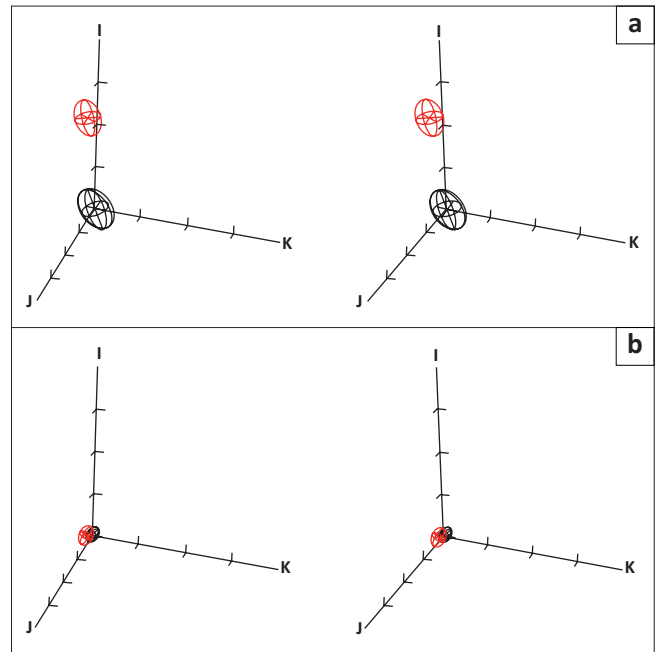


FIGURE 2: Stereo-pair scatter plots for central corneal power with 95% confidence ellipsoids for a single (a) keratoconic eye and a single (b) control eye. The axis length is 1 D, tick interval is 0.25 D and the origin is placed at the mean of the sample concerned. There were two measurement sessions for each participant in the study. Black represents Session one and red Session two. (Points are omitted to allow greater clarity with the small ellipsoids.) The intersection of confidence ellipsoids (or lack thereof) provides an indication of a change in the means over two measurement sessions.

$$\mathbf{v}' = \begin{bmatrix} F_{st} & F_{or} & F_{ob} \end{bmatrix} \text{ or } \mathbf{f}' = \begin{bmatrix} F_I & F_J & F_K \end{bmatrix} \quad [\text{Eqn 17}]$$

and therefore the mean coordinate vector can be given by:

$$\bar{\mathbf{v}} = \frac{1}{n} \sum \mathbf{v}_i \quad (\text{or } \bar{\mathbf{f}} = \frac{1}{n} \sum \mathbf{f}_i) \quad [\text{Eqn 18}]$$

and based on vector \mathbf{v} the variance–covariance of dioptric power is given by:

$$\mathbf{S} = \frac{1}{n-1} \sum_{i=1}^n (\mathbf{v}_i - \bar{\mathbf{v}})(\mathbf{v}_i - \bar{\mathbf{v}})' \quad (\text{or } \mathbf{S} = \frac{1}{n-1} \sum_{i=1}^n (\mathbf{f}_i - \bar{\mathbf{f}})(\mathbf{f}_i - \bar{\mathbf{f}})') \quad [\text{Eqn 19}]$$

According to Harris,¹¹: ‘...the mean is a value around which the sample clusters while the variance is a measure of the spread or dispersion of the cluster around the mean’. The mean and variance of a sample are statistical characteristics that are pertinent to finding correlations in data and drawing conclusions about the populations that the samples represent.

Harris^{6,9} discussed some of the methods used previously to average refractive error. He pointed out that while some of these methods led to the correct answer most times, there were instances where these methods were found to be incomplete or blatantly incorrect. An example of the *naive* mean was used to illustrate how analysis of data can be obscured.⁹ The example provided by Harris is as follows: the naive mean (obtained by averaging each component of a spherocylindrical power individually) of $1-1 \times 1$ and $1-1 \times 179$ was calculated to be $1-1 \times 90$, which was clearly wrong. With the use of matrices,^{4,15} an explicit method of

finding the mean of refractive errors was developed (see equation 16). The differences in means are a useful tool that can be used to identify changes over two measuring sessions for example. For instance, mean central corneal power measurements taken in Session one and Session two can be calculated and represented graphically with the aid of comets. Comets (see Figure 3) are drawn from the mean of the first to the mean of the second set of measurements for each eye. The length and direction of the comet provides a visual perspective on the changes in central corneal power from the first to the second session. Comets enable us to visibly track the change in means from the first set to second set of measurements. The longer the tail of the comet, the greater is the difference in the means between the first and second sessions.

In each of the comets in Figure 3, the dot represents the mean of the first set of 40 central corneal power measurements, and the end of the comet is the mean for the second set of 40 central corneal power measurements for each eye measured. In Figure 3a, which represents keratoconic eyes, the majority of the comets are more closely aligned to the antistigmatic plane. This implies that there are mostly astigmatic changes in the means over the two sessions. The control eyes are represented in Figure 3b, where it is evident that there is mostly a stigmatic change in means over the two measuring sessions. This is evident by almost all the comets aligning along the scalar axis. The length of the comets representing the keratoconic eyes is also mostly longer than the length of the comets representing the control eyes. This indicates greater variation in means for keratoconic eyes than for healthy control eyes.

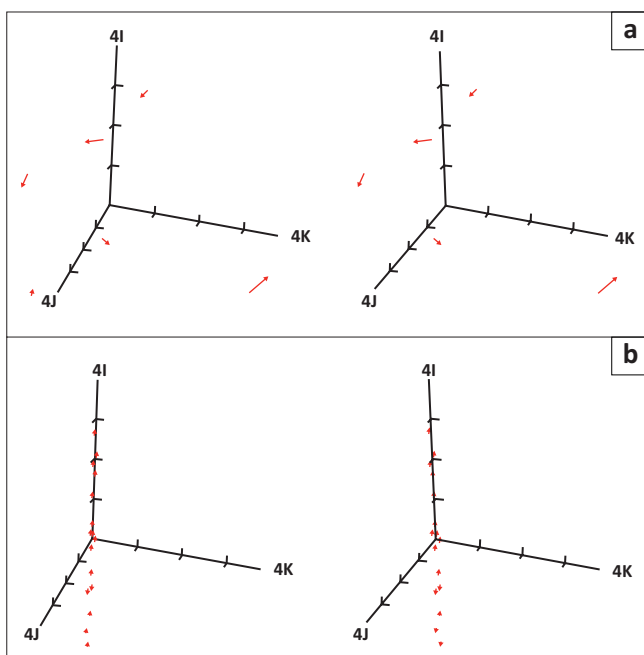


FIGURE 3: Stereo-pair scatter plots of comets joining the means of the measurements taken over two sessions: (a) for a group of eyes with keratoconus and (b) for a group of healthy control eyes. For each comet, the dot represents the mean of a set of 40 measurements taken in Session one for the eye concerned, and the comet ends at the mean of the measurements taken in Session two for the same eye. The origin is placed at the respective sample means. The axis lengths and tick intervals are 4 D and 1 D, respectively.

Saunders²⁶ asserted that dioptric power could not be squared, and hence the variance of a sample could not be calculated. Harris^{6,7,13,15} found this to be incorrect and showed for the first time that variance–covariance matrices could be calculated for dioptric power. Equation 19 calculates a symmetric 3×3 variance–covariance matrix with the unit D^2 :

$$\mathbf{S} = \begin{bmatrix} S_{11} & S_{12} & S_{13} \\ S_{21} & S_{22} & S_{32} \\ S_{31} & S_{32} & S_{33} \end{bmatrix} D^2.$$

There are six distinct entries in this matrix that describe the variances and covariance of a sample. The diagonal entries S_{11} , S_{22} and S_{33} characterise the variances for F_V , F_J and $F_{K'}$ respectively. The off-diagonal entries $S_{12} = S_{21}$, $S_{13} = S_{31}$ and $S_{23} = S_{32}$ characterise the covariances between F_V and F_J , F_V and $F_{K'}$ and F_J and $F_{K'}$ respectively. The variances and covariances across the meridians of one or more eyes can be graphically represented by means of a polar profile.⁴²

Polar profiles of variance–covariance

The variances and covariances across the meridians of one or more eyes can be graphically represented using a polar profile (Figure 4) in which the reference meridian θ is from 0° to 180° . The solid line in the plot represents the curvital variance profile, which is the only profile, required to adequately describe the curvital nature of dioptric power variation across the meridians of the eye. The curvital variance profile is accompanied by the scaled torsional

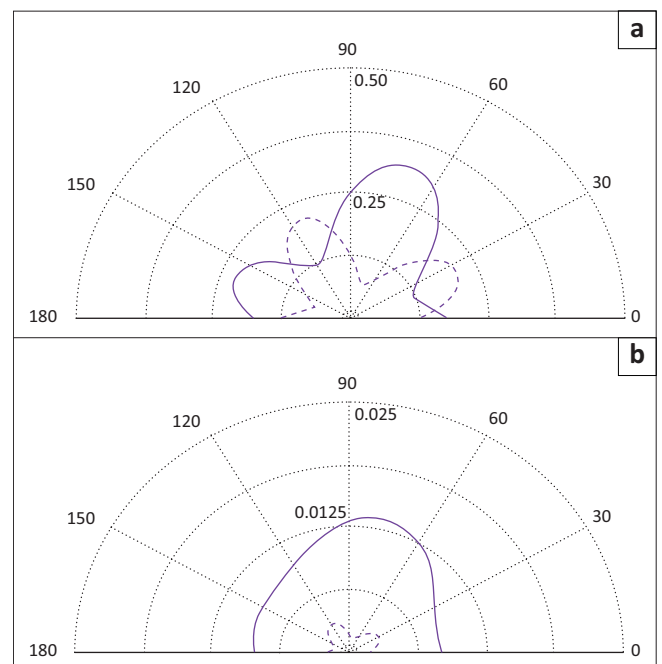


FIGURE 4: Polar profiles of variation in central corneal power of (a) a keratoconic eye and (b) a control eye. The solid curve is curvital and the dash is torsional. The radial scale and outer circle (in dots) are set at $0.5 D^2$ and $0.025 D^2$ for (a) and (b), respectively. For the keratoconic eye, the meridian of greatest curvital variance is near 70° and torsional variance is maximal near 115° , whereas the control eye displays maximum curvital variation near 80° and maximum torsional variation near 120° . The variances for the control eye are much smaller than that of the keratoconic eye.

variance profile (the dashed curve), which describes the torsional nature of dioptric power variation across the meridians of the eye and makes the nature of dioptric power variation easier to visualise and quantify.

If variation is purely scalar (spherical), then the scaled torsional variance profile will be reduced to a point at the origin of the polar plot, and the curvital variance profile becomes a semi-circle of constant radius. When variation is uniform across all meridians of the eye both profiles take on a semi-circular shape. If variation is non-uniform, then profiles depart from being semi-circles. The torsional variance profile often assumes the shape of a pair of 'rabbit ears' as described by Van Gool⁴² and seen in Figure 4. The characteristics of the rabbit ears provide useful information about dioptric power variation across the meridians of the eye. The pair of ears is symmetrical and always 90° apart and the maximum and minimum magnitude can be determined from the position of the ears. As established by Van Gool⁴² and also shown by Gillan,³³ there appears to be a strong correlation between the position of the rabbit ears and the major axis of the corresponding distribution ellipsoid. If, for example, the rabbit ears orientate symmetrically about the 90° axis, then one can expect to find the major axis of the corresponding distribution ellipsoid orientated parallel to the astigmatic plane when viewed straight down the stigmatic axis. The following two examples are provided to illustrate how central corneal power varies across all the meridians of the eye and not just within the principal meridians as indicated by many researchers who analyse this sort of data only along the horizontal and/or vertical meridians.

For Figure 4, each polar plot contains the polar profiles for (1) central corneal power measurements taken on a single keratoconic eye and (2) central corneal power measurements taken on a single control eye. In each plot, the solid blue curve represents the curvital variance profile and the dashed blue curve represents the scaled torsional variance profile for the dioptric power measurements of the first session. The meridians are labelled from 0° to 180° in 30° intervals for all polar plots; however, the scale of the plots differ for optimal representation and is specified for each eye.

Figure 4b shows that for the control eye, the scaled torsional variance profile (dashed curve) appears within the curvital variance profile (solid curve); therefore, this eye experiences greater curvital dioptric power variation than torsional dioptric power variation. Contrary to that, the keratoconic eye (Figure 4a) exhibits greater amounts of torsional variation than for the control eye and especially when the differences in radial scales are taken into consideration. This is evident by the dashed line (torsional variance) that sometimes even extends beyond the solid curve (curvital variance).

Note that the scales are different for the two polar plots, and thus they cannot be so easily compared directly in terms of magnitude of variation. However, on closer inspection of the figures, one would note that the keratoconic eye exhibits the most variation and the control eye exhibits the least variation,

irrespective of type of variation (i.e. curvital or torsional). The use of polar plots highlights clearly that dioptric power variation is not isolated to only principal meridians or the horizontal and vertical meridians (180° and 90°) and that there is also a torsional component of variation (albeit small in healthy eyes) that accompanies the curvital variation. This is an important finding and this method of analysis (i.e. polar plots of variance) tends to be ignored or misunderstood in more traditional dioptric power analysis.

Multivariate hypothesis testing

Hypothesis testing forms an integral part of statistical analysis. It allows one to make assumptions at a certain level of confidence regarding a population. The multivariate test statistic w is a generalisation of the univariate t^2 statistic. Details on these statistics and their respective definitions are provided elsewhere¹⁵ for a more comprehensive understanding. Hypothesis tests are conducted on the variance-covariances and means for all sets of measurements. For example, the equality of variance-covariances and means for a set of dioptric power measurements taken in a first session can be tested against the variance-covariances and means for the dioptric power measurements taken in a second session. For μ_v and Σ_v representing the mean and the variance-covariances of a population of dioptric power data, the hypothesis tests are as follows:^{15,19}

For testing means, the null hypothesis

$$H_0: \mu_v = \mu_v^0$$

is tested against the alternative hypothesis

$$H_1: \mu_v \neq \mu_v^0$$

and the test statistic is given by

$$w = (\bar{v} - \mu_v^0)' S_{vv}^{-1} (\bar{v} - \mu_v^0) n(n-m) / (m[n-1]). \quad [\text{Eqn 20}]$$

The null hypothesis is rejected if the test statistic is greater than or equal to the critical value, that is,

$$w \geq F_{\alpha, m, n-m}$$

in which F is found in Snedecor's F -distribution chart by α , m and $n - m$, which represent the level of significance, degrees of freedom in the numerator and degrees of freedom in the denominator, respectively.

For example, $\alpha = 0.05$, $m = 3$ and $n - m = 76$, which resulted in $F = 2.725$.

For testing variance-covariances, the null hypothesis

$$H_0: \Sigma = \Sigma_0$$

is tested against the alternative hypothesis

$$H_1: \Sigma \neq \Sigma_0$$

and the test statistic is given by

$$L = (N - 1 [\log\{\det\Sigma_0\} - \log\{\det S\} + \text{tr}\{S\Sigma_0^{-1}\}] - p). \quad [\text{Eqn 21}]$$

The null hypothesis is rejected if the test statistic is greater than the critical value, that is,

$$L > \chi^2_{\alpha, p(p+1)/2}$$

where χ^2 can be found in the chi square distribution table. For example, $\alpha = 0.05$ and the critical value is 12.592.

The underlying assumption when conducting hypothesis tests on means is that $\Sigma = \Sigma_0$. An adequate alternative for cases where $\Sigma \neq \Sigma_0$ has not been found, and this is referred to as the Behrens–Fisher problem.¹⁹

Multivariate normality

Multivariate statistical analysis is generally based on the assumptions of random selection and multivariate normality of samples. Multivariate normality is modelled with respect to the bell-shaped curve and the associated assumptions that the distribution is continuous, perfectly symmetrical, unskewed and mesokurtic and that the mean, median and mode are all equal.⁴³ Because of the nature of spherocylindrical data one or more of these underlying assumptions are not always met. While the solution to the problem has not yet been discovered and therefore cannot be circumvented, one continues with the statistical analysis and is prudent with the interpretation of the results.

Multivariate normality can be investigated with the aid of various tools such as skewness and kurtosis, identification

of possible outliers (using Mahalanobis distances; Figure 5) and the comparison of means and medians of the samples. An online statistical tool, WebPower statistical power analysis online,⁴⁴ can be used to calculate the skewness and kurtosis for multivariate samples such as dioptric power. The developers of this programme discuss how the calculations are done to arrive at a *b*-value, *z*-value and an associated *p*-value for skewness and kurtosis. The details thereof are beyond the scope of this review and the interested reader is referred to Cain et al.⁴⁵ Possible outliers are assumed atypical in the sample and may be subjectively identified as one or more data points that appear to be far removed from the cluster of data. The Mahalanobis distance is an objective method to quantify the distance so that one can identify possible outliers more accurately. Figure 4 illustrates an example of the Mahalanobis distances that were calculated for a multivariate sample.

Conclusion

Multivariate methods of analysis are especially pertinent when investigating keratometric and refractive power data, which is fundamentally trivariate in nature. With the aid of multivariate methods of analysis, keratometric and refractive data would be represented in their entirety; that is, all three components of sphere, cylinder and axis would be used to plot data on three-dimensional stereo-pairs that have distinct advantages, for data visualisation and quantitative analysis in comparison to other methods that use vector analysis in two-dimensional space only. Although some of these methods may seem complicated at first, this review offers a simplified overview of some multivariate

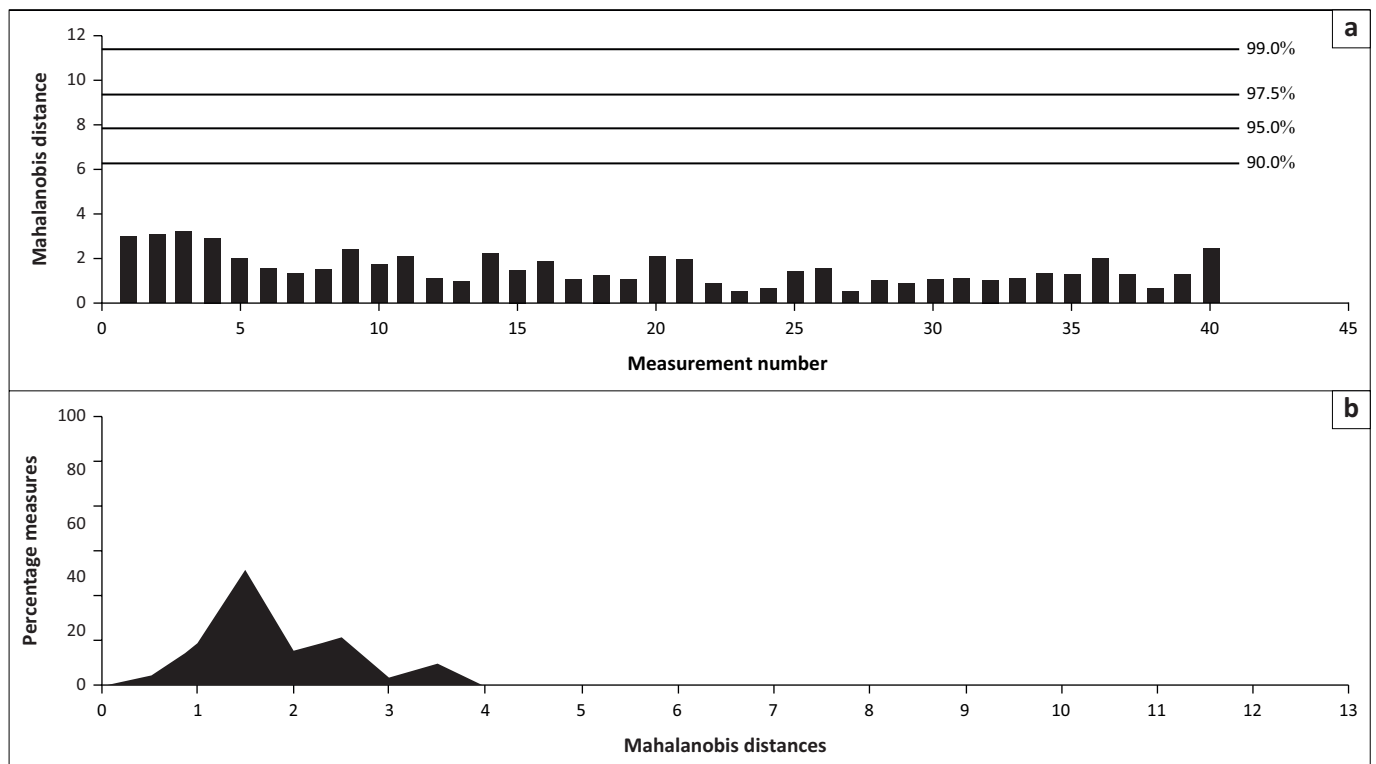


FIGURE 5: The Mahalanobis distances for central corneal power measurements.⁴¹ None of the 40 measurements for a single eye reach the critical distance (or percentage) that would imply possible outliers ($\leq 90\%$).

methods of analysis that are available to analyse dioptric power holistically.

Acknowledgements

Competing interests

The authors declare that they have no financial or personal relationships that may have inappropriately influenced them in writing this article.

Authors' contributions

E.C. and A.R. contributed equally to this work.

Ethical considerations

Approval to conduct the study was obtained from the Research Ethics Committee of the Faculty of Health Sciences of the University of Johannesburg, South Africa (ethical clearance number: REC-241112-035)

Funding information

This study was funded by the Thuthuka grant (TTK160519165562) from the National Research Foundation in South Africa.

Data availability

Data sharing is not applicable to this article as no new data were created or analysed in this study.

Disclaimer

The views and opinions expressed in this article are those of the authors and do not necessarily reflect the official policy or position of any affiliated agency of the authors.

References

- Long WF. A matrix formalisation for decentration problems. *Am J Optom Physiol Opt.* 1976;53(1):27–33. <https://doi.org/10.1097/00006324-197601000-00005>
- Keating MP. An easier method to obtain sphere, cylinder and axis from an off-axis dioptric power matrix. *Am J Optom Physiol Opt.* 1980;57(10):734–737. <https://doi.org/10.1097/00006324-198010000-00007>
- Keating MP. A system matrix for astigmatic optical systems: Introduction and dioptric power relations. *Am J Optom Physiol Opt.* 1981;58(10):810–819. <https://doi.org/10.1097/00006324-198110000-00006>
- Keating MP. On the use of matrices for the mean value of refractive errors. *Ophthal Physiol Opt.* 1983;3(2):201–203. <https://doi.org/10.1111/j.1475-1313.1983.tb00599.x>
- Harris WF. The matrix representation of dioptric power. Part 1: An introduction. *S Afr Optom.* 1988;47(4):19–23.
- Harris WF. Algebra of spherocylinders and refractive errors, and their means, variance, and standard deviation. *Am J Optom Physiol Opt.* 1988;65(10):794–802. <https://doi.org/10.1097/00006324-198810000-00003>
- Harris WF. Squaring the spherocylinder, the equivalent of squaring the refractive power matrix. *Ophthal Physiol Opt.* 1988;8(4):458–459. <https://doi.org/10.1111/j.1475-1313.1988.tb01185.x>
- Harris WF. The matrix representation of dioptric power. Part 2: Adding obliquely-crossed spherocylinders. *S Afr Optom.* 1989;48:22–24.
- Harris WF. The matrix representation of dioptric power. Part 3: The average refractive error. *S Afr Optom.* 1989;48:81–88.
- Harris WF. Simplified rational representation of dioptric power. *Ophthal Physiol Opt.* 1989;9(4):455. <https://doi.org/10.1111/j.1475-1313.1989.tb00952.x>
- Harris WF. The mean and variance of samples of dioptric powers: The basic calculations. *Clin Exp Optom.* 1990;73:89–92.
- Harris WF. Elements of the dioptric power matrix and the concept of torsional power: A reinterpretation. *Optom Vis Sci.* 1990;67(1):36–37. <https://doi.org/10.1097/00006324-199001000-00008>
- Harris WF. Direct, vec and other squares, and sample variance-covariance of dioptric power. *Ophthal Physiol Opt.* 1990;10(1):72–80. <https://doi.org/10.1111/j.1475-1313.1990.tb01110.x>
- Harris WF. Mean of a sample of equivalent dioptric powers. *Optom Vis Sci.* 1990;67(5):359–360. <https://doi.org/10.1097/00006324-199005000-00010>
- Harris WF. Statistical inference on mean dioptric power: Hypothesis testing and confidence regions. *Ophthal Physiol Opt.* 1990;10(4):363–372. <https://doi.org/10.1111/j.1475-1313.1990.tb00883.x>
- Harris WF. Representation of dioptric power in Euclidean 3-space. *Ophthal Physiol Opt.* 1991;11(2):130–136. <https://doi.org/10.1111/j.1475-1313.1991.tb00212.x>
- Harris WF. Statistical inference on mean dioptric power: Asymmetric powers and singular covariance. *Ophthal Physiol Opt.* 1991;11(3):263–269. <https://doi.org/10.1111/j.1475-1313.1991.tb00542.x>
- Harris WF. Meridional profiles of variance-covariance of dioptric power part 1. The basic theory. *Ophthal Physiol Opt.* 1992;12(4):467–470. <https://doi.org/10.1111/j.1475-1313.1992.tb00317.x>
- Harris WF. Testing hypotheses on dioptric power. *Optom Vis Sci.* 1992;69(11):835–845. <https://doi.org/10.1097/00006324-199211000-00002>
- Harris WF. Keating's asymmetric dioptric power matrices expressed in terms of sphere, cylinder, axis and astigmatism. *Optom Vis Sci.* 1993;70(8):666–667. <https://doi.org/10.1097/00006324-199308000-00014>
- Harris WF. Dioptric power: Its nature and its representation in three- and four-dimensional space. *Optom Vis Sci.* 1997;74(6):349–366. <https://doi.org/10.1097/00006324-199706000-00018>
- Harris WF. Astigmatism. *Ophthal Physiol Opt.* 2000;20(1):11–30. <https://doi.org/10.1046/j.1475-1313.2000.00484.x>
- Harris WF. Clinical measurement, artefact, and data analysis in dioptric power space. *Optom Vis Sci.* 2001;78(11):839–845. <https://doi.org/10.1097/00006324-200111000-00014>
- Harris WF. Reduction of artefact in scatter plots of spherocylindrical data. *Ophthal Physiol Opt.* 2005;25(1):13–17. <https://doi.org/10.1111/j.1475-1313.2004.00249.x>
- Harris WF. Power vectors versus power matrices, and the mathematical nature of dioptric power. *Optom Vis Sci.* 2007;84(11):1060–1063. <https://doi.org/10.1097/OPX.0b013e318157acbb>
- Thibos LN, Wheeler W, Horner D. Power vectors: An application of Fourier analysis to the description and statistical analysis of refractive error. *Optom Vis Sci.* 1997;74(6):367–375. <https://doi.org/10.1097/00006324-199706000-00019>
- Saunders H. The impossibility of squaring the spherocylinder. *Ophthalmol Physiol Opt.* 1985;5(2):95. <https://doi.org/10.1111/j.1475-1313.1985.tb00642.x>
- Rubin A. Short-term variation of refractive behaviour in human eyes. MPhil dissertation. Johannesburg: Rand Afrikaans University; 1993.
- Cronje-Dunn S. Short-term keratometric variation in the human eye. MPhil dissertation. Johannesburg: Rand Afrikaans University; 1995.
- Cronje-Dunn S, Harris WF. Keratometric variation: The influence of a fluid layer. *Ophthalmol Physiol Opt.* 1996;16(3):234–236. <https://doi.org/10.1046/j.1475-1313.1996.95001174.x>
- Cronje S, Harris WF. A comparison of keratometric variation in manual and automatic keratometry. *S Afr Optom.* 1999;58:31–39.
- Du Toit I. The effect of physical exercise on keratometric variation in the human eye. MPhil dissertation. Johannesburg: Rand Afrikaans University; 2001.
- Gillan WDH. The effects of light and dark conditions on refractive behaviour. DPhil thesis. Johannesburg: Rand Afrikaans University; 2004.
- Gillan WDH. Variation in surface power and thickness of a moderately keratoconic cornea. *S Afr Optom.* 2008;67:4–10.
- Blendowske R, Hans-Heinrich Fick: Early contributions to the theory of astigmatic systems. *S Afr Optom.* 2003;62:105–110.
- Malan DJ. Applying the dioptric power matrix: Computer programmes for practical calculations. *S Afr Optom.* 1989;48:89–90.
- Malan DJ. Computer programme for calculating mean refractive error. *S Afr Optom.* 1990;49:83–85.
- Malan DJ. Dioptric power data analysis: Computer implementation of graphical methods with clinical examples. *S Afr Optom.* 1993;52:84–90.
- Harris WF, Malan DJ, Rubin A. The distribution of dioptric power: Ellipsoids of constant probability density. *Ophthalmol Physiol Opt.* 1991;11(4):381–384. <https://doi.org/10.1111/j.1475-1313.1991.tb00239.x>
- Harris WF, Malan DJ, Rubin A. Ellipsoidal confidence regions for mean refractive state. *Optom Vis Sci.* 1991;68(12):950–953. <https://doi.org/10.1097/00006324-199112000-00007>
- Chetty E. A multivariate analysis of short-term variation of keratometric behaviour, refractive state and pachymetry in keratoconic corneas. DPhil thesis. Johannesburg: University of Johannesburg; 2019.
- Van Gool RD. Refractive variation under accommodative demand. DPhil thesis. Johannesburg: Rand Afrikaans University; 2000.
- Hair JF Jr, Black WC, Babin BJ, Anderson RE. *Multivariate data analysis: A global perspective.* Hoboken, NJ: Pearson; 2010.
- Zhang Z, Yuan KH. *Practical statistical power analysis using Webpower* [homepage on the Internet]. Granger, IN: ISDSA Press; 2018 [cited 2018 Jul 18]. Available from: <https://webpower.psychstat.org>.
- Cain MK, Zhang Z, Yuan KH. Univariate and multivariate skewness and kurtosis for measuring nonnormality: Prevalence, influence and estimation. *Behav Res Met.* 2017;49(5):1716–1735. <https://doi.org/10.3758/s13428-016-0814-1>